Effect of Noncovalent Interactions on Conformers of the *n*-Butylbenzene Monomer Studied by Mass Analyzed Threshold Ionization Spectroscopy and Basis-set Convergent *ab initio* Computations

Xin Tong,[†] Jiří Černý,[†] and Klaus Müller-Dethlefs*[,†,‡]

The Photon Science Institute, Alan Turing Building, the School of Chemistry, and the School of Physics and Astronomy, The University of Manchester, Manchester, M13 9PL, U.K.

Caroline E. H. Dessent

Department of Chemistry, Universtiy of York, Heslington, York YO10 5DD, U.K.

Received: November 19, 2007; Revised Manuscript Received: March 15, 2008

Two conformational isomers of the aromatic hydrocarbon *n*-butylbenzene have been studied using two-color MATI (mass analyzed threshold ionization) spectroscopy to explore the effect of conformation on ionization dynamics. Cationic states of g*auche*-conformer III and *anti*- conformers IV were selectively produced by two-color excitation *via* the respective S_1 origins. Adiabatic ionization potentials of the *gauche*- and *anti*-conformations were determined to be 70146 and 69872 ± 5 cm^{-1} respectively. Spectral features and vibrational modes are interpreted with the aid of MP2/cc-pVDZ *ab initio* calculations, and ionization-induced changes in the molecular conformations are discussed. Complete basis set (CBS) *ab initio* studies at MP2 level reveal reliable energetics for all four *n*-butylbenzene conformers observed in earlier two-color REMPI (resonance enhanced multiphoton ionization) spectra. For the S_0 state, the energies of conformer III, IV and V are above conformer I by 130, 289, 73 cm^{-1}, respectively. Furthermore, the combination of the CBS calculations with the measured REMPI, MATI spectra allowed the determination of the energetics of all four conformers in the S_1 and D_0 states.

1. Introduction

Much of chemistry is, naturally, concerned with the covalent bonds that hold molecules together. Most chemical reactions involve the breaking of such bonds and the forming of new ones. However, before any such chemical reaction can begin, the two moieties must approach each other within a critical distance of one another. This approach is controlled by the forces between them or the molecular interactions between the moieties, known as noncovalent interactions.[1–4] These noncovalent interactions are important not only as a precursor to a chemical reaction between species but also with respect to the formation of molecular clusters about one another or as influencing factors in the structure within molecular monomer.[5–12] In this work, *n*-butylbenzene (BB) is investigated to understand the impact of noncovalent interactions on the energetics of its conformers. This discussion is continued for its rare gas cluster in the following paper.[13]

In our previous study, the $S_1 \leftarrow S_0$ and $D_0 \leftarrow S_1$ transitions of two conformers of BB (neutral ground state, S_0; neutral excited state, S_1; cationic ground state, D_0) were studied in a skimmed supersonic jet expansion with REMPI (resonance enhanced multiphoton ionization) and MATI (mass analyzed threshold ionization) spectroscopy.[14] The spectra obtained were discussed in the context of conformer specific ionization-induced geometry changes, and complementary subsequent work relating to partially rotationally resolved zero electron kinetic energy (ZEKE) spectra was analyzed with a spectator orbital model.[15]

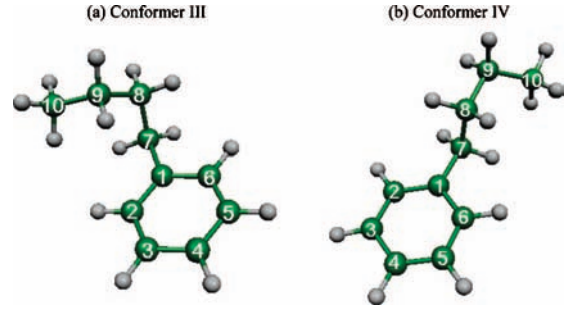

Figure 1. Geometric structures of the S_0 state conformers (a) III (*gauche*) and (b) IV (*anti*) of BB calculated at the MP2/cc-pVTZ level, with carbon atom labels.

These studies provided new insights into the importance of electronic structure changes in threshold ionization spectroscopies and illustrated that the relatively small difference in geometry between two molecular conformers can have a dramatic effect on the ionization dynamics.

Although four stable neutral conformers (I, III, IV and V) of BB were previously observed in the early (1 + 1′) REMPI spectrum,[14,16] only the two dominant conformers (I and V) were studied by MATI spectroscopy due to the signal-to-noise ratio for conformers III and IV being too poor to produce valuable spectroscopic information.[14] With improvements to our experimental system, particularly with more than a 1 order enhancement of the output power of the ionization dye laser, the opportunity arose to reinvestigate BB isomers III and IV.

Conformer III (Figure 1a) corresponds to another *gauche*-conformer similar to conformer I,[14] where the methyl group

* Corresponding author. E-mail: K.Muller-dethlefs@manchester.ac.uk.
† The Photon Science Institute and the School of Chemistry.
‡ School of Physics and Astronomy.

10.1021/jp710997q CCC: $40.75
Published on Web 06/06/2008

(C10) at the end of hydrocarbon tail of the molecule is oriented along the aromatic ring plane, away from the aromatic ring. Compared with the *gauche*-conformer geometric structure of conformer I, C9 is rotated up and away from the aromatic ring. Conformer IV (Figure 1b) represents an *anti*-conformer similar to conformer V, where, although the tail is oriented away from the ring in *anti*-geometry, the end methyl group turns back. Therefore, there are only minor geometric differences among the *gauche*-conformers and among the *anti*-conformers.

Our early study has shown a strong correspondence between relative energies and minor geometric differences. The *gauche*-conformer BB-I is more stable than *anti*-conformers BB-V due to the noncovalent interaction between one hydrogen atom bonded on carbon atom C9 and the aromatic π ring electrons. This conclusion may not be always suitable to apply for both *gauche*-conformers, because such a weak noncovalent interaction can be influenced by the orientation of the CH_n group in the floppy alkyl chain. To determine the relative energies between them becomes a challenge for theory, because, as reported earlier, the relative energy difference between BB-I and BB-V is only 38 cm^{-1}, which is obtained by experiment. For systems of such size, it is also computationally expensive to use high level theory with a high level basis set. Therefore, in this work, we employ a basis set extrapolation method that allows us to use a medium size basis set to close the gap between theoretical and experimental results.

Actually, basis set convergence and extrapolation are among the most important issues of contemporary molecular *ab initio* theory.[17–20] It is well-known that convergence of the correlation part is significantly slower than that of the Hartree−Fork (HF) part. This suggests, when studying the basis set convergence of the energy, one should treat the HF and correlation parts separately. In recent years, several different forms of extrapolation, including the exponential and the power forms, have been developed. Our economic extrapolation scheme to the complete basis follows the recipe of Helgaker.[17] In his paper, several ideas on extrapolations suggested elsewhere were connected. In this work, the two-point linear exponential dependence of the HF energy was employed:

$$E_X^{\mathrm{HF}} = E_{\mathrm{CBS}}^{\mathrm{HF}} + A\mathrm{e}^{-\alpha X} \quad (1)$$

where E_X^{HF} and $E_{\mathrm{CBS}}^{\mathrm{HF}}$ are HF energies for the basis set with angular momentum X and for the complete basis set, respectively. The parameters α are fitted by Helgaker ($\alpha = 1.43$ for $X = 3$ and $\alpha = 1.54$ for $X = 4$). The correlation energy is extrapolated by a two-point power dependence formula:

$$E_X^{\mathrm{corr}} = E_{\mathrm{CBS}}^{\mathrm{corr}} + BX^{-3} \quad (2)$$

where E_X^{corr} and $E_{\mathrm{CBS}}^{\mathrm{corr}}$ are correlation energies for the basis set with angular momentum X and for the complete basis set, respectively. The coefficient A in formula 1 and B in formula 2 are also determined by the two-point extrapolation.

2. Experimental Setup

The experimental apparatus has been described in detail earlier[21] and will be discussed only briefly here. BB (Lancaster Synthesis, 99% purity) was introduced *via* an internal sample holder located directly behind the valve and expanded in a supersonic jet through a 0.8 mm diameter nozzle (General Valve), using argon as a backing gas at a stagnation pressure of 2 bar to generate a sufficient yield of monomers. The rotational temperature of the molecule is approximately 2 K after the expansion.[22] The molecular beam interacts with the counter propagating, frequency-doubled outputs of two Nd:YAG pumped dye lasers (Radiant Narrowscan) using Coumarin 153 and Sulfurhodamin B. Two-color ($1 + 1'$) REMPI spectroscopy was used to obtain the S_1 state spectrum, with the second photon's energy controlled to minimize spectral contamination *via* fragmentation of higher mass species.[12] The pulse sequences, timings and field strengths used to obtain the REMPI spectra are identical to those in ref 21.

MATI spectroscopy was used to obtain the threshold ionization spectra of BB, because it provides equivalent resolution to ZEKE spectroscopy with the advantage of unambiguous mass-selectivity.[23,24] In addition, although the absolute signal intensities in a MATI experiment are generally lower than in the analogous ZEKE experiment, MATI spectra can display a considerably higher signal-to-noise ratio due to mass selective detection. The pulse sequences, timings and field strengths used to obtain the MATI spectra are identical to those in ref 24. Laser wavelengths were calibrated in vacuum wavenumbers by simultaneously recording iodine spectra.[25] Ionization energies are field corrected using $\Delta E\ (\mathrm{cm}^{-1}) = 4[F\ (\mathrm{V/cm})]^{1/2}$, where F presents the field strength.[26]

3. Computational Details

To compare with the experimental work, series of *ab initio* calculations were performed at the different levels of theory for S_0 and D_0 states of all four conformers by using Gaussian 03, version C.02.[27] The RMP2/cc-pVTZ level of calculation is used to determine their geometries in the S_0 state. Previous studies indicate the smallest correlation-consistent polarized valence basis sets, cc-pVDZ, may not give a sufficiently accurate geometry to perform an extrapolation toward the complete basis set energy.[28] Because it is well-known that the MP2 method overestimates dispersion, an augmented basis set is not used for geometry calculation because this overestimation of dispersion in MP2 seriously undermines the gradient calculation for geometry optimization.[28] In addition, unscaled frequency calculation were carried out to ensure that optimized structures were identified as local minima and zero point energies were taken account for all total energies.

To perform the extrapolation to CBS, total energies for all isomers are deduced from aug-cc-pVDZ (aDZ), aug-cc-pVTZ (aTZ) and aug-cc-pVQZ (aQZ). Due to the rapid increasing computational cost, it is beyond our reach to perform higher order basis set calculation beyond aQZ. As stated above, the augmented basis set is not suitable for geometry optimization; however, it does not damage the comparison among the four isomers because the MP2 overestimation of total energy is the same for all of them and thus cancels out. More important, the augmented basis set will recover very subtle noncovalent interaction differences between aromatic ring and alkyl side chain among these conformers, which ideally meet our requirement.

To aid the assignment of the MATI spectra, we also performed frequency calculations for the cationic state. The calculation of the cationic state is always a big challenge for *ab initio* methods because of possible spin contamination and heavy computational cost. Here, only the UMP2/cc-pVDZ level is used for the cation. Furthermore, to compare the calculated ionization energy with experiment, we use the same level basis set (cc-pVDZ) for all neutral ground states to obtain ionization energies. Although this level may be inefficient compared with our extrapolation method requirement at S_0 states, but one can see those calculations indeed gives very good agreement with our experimental results in section 4.3.

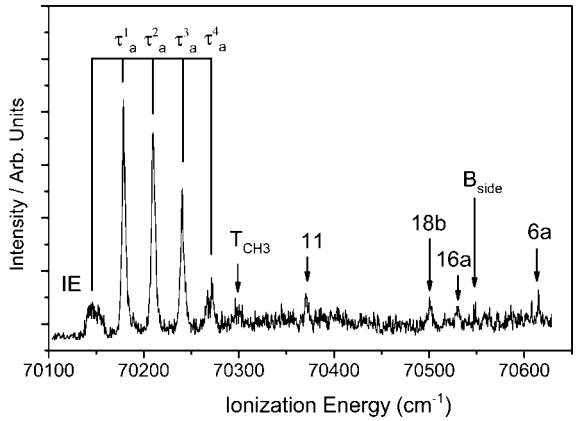

Figure 2. Two-color (1 + 1′) MATI spectrum of conformer III of BB recorded *via* the $S_1 0^0$ intermediate state. Assignments of the τ_a torsion of the side chain, the T_{CH_3} inter-rotation, the 11, 18b, 16a, 6a of aromatic ring vibration modes and the B_{side} side chain bending mode are included on the spectrum.

4. Spectroscopic Study of *n*-Butylbenzene III and V

A two-color (1 + 1′) REMPI spectrum of jet-cooled BB was presented in our previous study and analyzed in detail.[14] It reveals that the $S_1 0^0$ bands of conformers I, III, IV and V appear at 37513, 37514, 37572 and 37575 ± 0.5 cm^{-1}.

4.1. MATI Spectrum of *n*-Butylbenzene Conformer III. Figure 2 displays the MATI spectrum of the *gauche*-conformer III of BB obtained *via* the $S_1 0^0$ origin at 37514 cm^{-1}.

Although the first peak appearing at 70146 ± 5 cm^{-1} is not the dominant peak in this spectrum, and because no additional spectral features were observed in the lower energy spectral range (with good jet cooling and a narrow band excitation laser), we assign it as the adiabatic ionization energy (IE). A number of very strong features appear in the low ion internal energy range of 32, 63, 95 and 125 cm^{-1} in this MATI spectrum, whereas the features in the higher energy range appear more weakly at 150, 224, 354, 383, 402 and 469 cm^{-1}.

Figure 3 displays the harmonic vibrational frequencies of the nine lowest frequency modes of the D_0 state of conformer III obtained at the UMP2/cc-pVDZ level. Surprisingly, unlike the normal mode vibrational results for BB-I and BB-V reported early,[14] the alkyl chain vibrational modes are significantly separated from the aromatic ring vibrational modes. For the higher energy range (above 370 cm^{-1}), the BB-III cation conformer displays very similar aromatic ring vibrational modes (11, 18b, 16a and 6a) as the phenol cation and there is little mixing of chain and ring modes.[29] Two new pure alkyl chain modes, which are the methyl group rotor T_{CH_3} and the alkyl chain bend mode B_{side}, appear in the calculated results of the BB-III cation conformer but not in either the BB-I or BB-V cation.[14] Tentative assignments are included in Figure 2. Because conformer III adopts a C_1 symmetry structure, there are no symmetry restrictions on the vibrational modes that appear in the conformer V MATI spectrum.[14]

By comparison with the *ab initio* results, we assign the most intense vibrational feature at 32 cm^{-1} to the C_1-C_7 torsion τ_a, with a series of progression features appearing at 63, 94 and 125 cm^{-1}. The weak peak at 150 cm^{-1} is assigned to the alkyl chain T_{CH_3} which is not observed in the BB-I and BB-V cationic states.[14] Four aromatic ring modes observed at 224, 354, 383 and 469 cm^{-1} are assigned to the long axis ring bend mode 11, the in plane chain-ring-bend mode 18b, the tilt axis ring bend mode 16a and the ring stretch mode 6a. The interesting peak located at 402 cm^{-1} is assigned to the pure alkyl chain bend mode B_{side}. This mode is not observed in conformer I and V, which have highly mixed side chain and ring modes. The weak IE peak, the strong progression of τ_a and the lack of other combination features suggest that upon ionization there is a significant change of geometry. It is very likely that this change involves the relative structure between the alkyl side chain and the aromatic ring. All the observed internal rotational and vibrational features of the conformer I cation are summarized in Table 1.

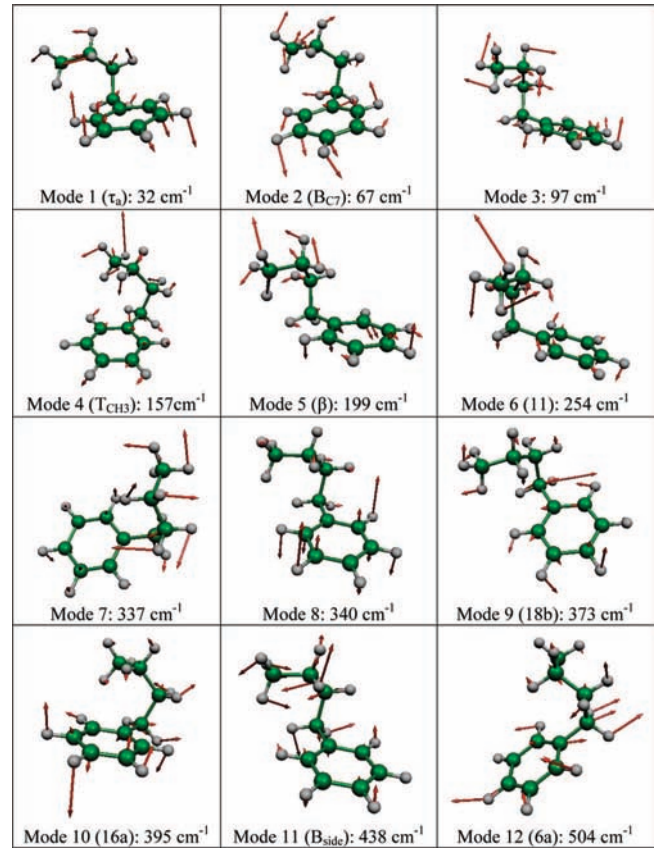

Figure 3. First twelve vibrational modes of the D_0 state of conformer III of BB calculated at the UMP2/cc-pVDZ level.

TABLE 1: Frequencies (in cm^{-1}) and Assignments of the Vibrational Bands Observed in the MATI Spectrum of Conformer III of BB

peak position	ion internal energy	intensity[a]	assignment	MP2/cc-pVDZ
70146	0	m	IE	
70178	32	s	τ_a	32
70209	63	s	τ_a^2	
70241	95	s	τ_a^3	
70271	125	m	τ_a^4	
70296	150	vw	T_{CH_3}	157
70370	224	w	11	254
70500	354	w	18b	373
70529	383	w	16a	395
70548	402	w	B_{side}	438
70615	469	w	6a	504

[a] Intensities are denoted as s = strong, m = medium, w = weak and vw = very weak.

4.2. MATI Spectrum of *n*-Butylbenzene Conformer IV. Figure 4 displays the MATI spectrum of the *anti*-conformer IV of BB obtained *via* the $S_1 0^0$ vibrationless origin. The prominent feature at 69872 ± 5 cm^{-1} is again assigned to the IE because no additional spectral features were observed in the lower energy

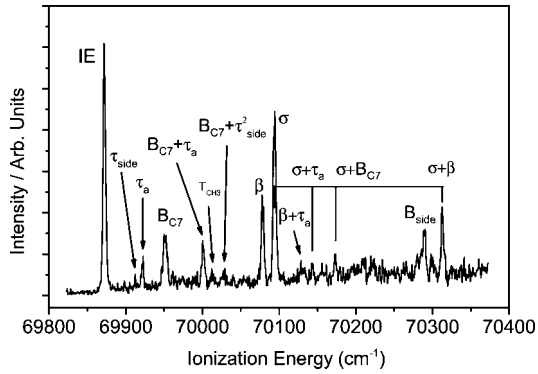

Figure 4. Two-color (1 + 1′) MATI spectrum of conformer IV of BB recorded *via* the $S_1 0°$ intermediate state. Assignment of the τ_{side} and τ_a torsions, the B_{C7} bend, the β bend, the σ stretching and the B_{side} bend modes and their combinations are included on the spectrum.

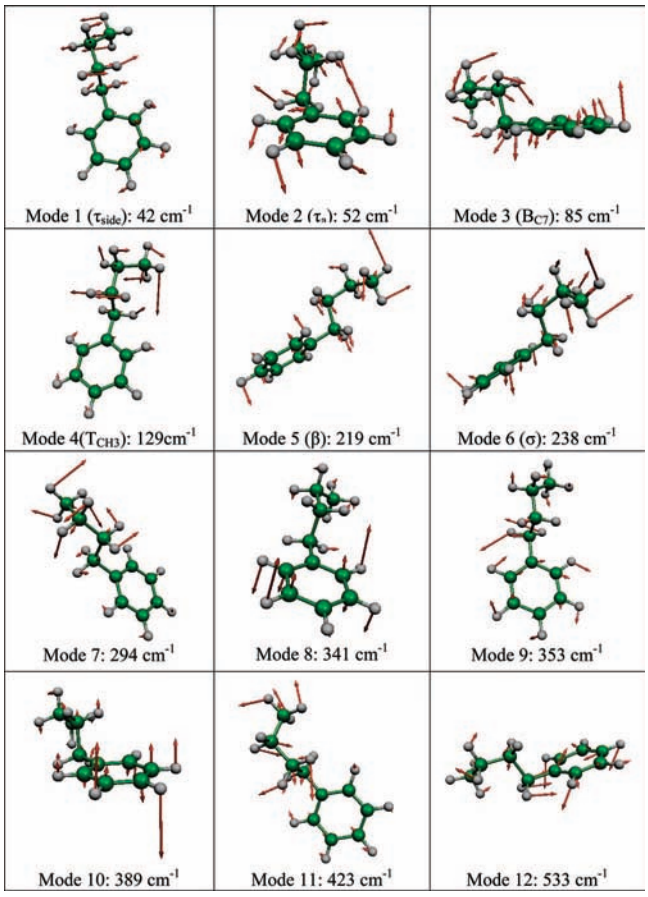

Figure 5. First twelve vibrational modes of the D_0 state of conformer IV of BB, calculated at the UMP2/cc-pVDZ level.

spectral range. The ionization energies of *anti*-conformers IV and V are lower than *gauche*-conformers I and III. This is due to the noncovalent repulsive interaction between the hydrogen atom bonded with the C9 carbon atom and the positively charged aromatic ring. Similar relative ionization energies have been observed for other alkylbenzene cations, such as toluene,[30] ethylbenzene[31] and *n*-propylbenzene.[32]

A number of internal rotation and vibrational features are again evident in the MATI spectrum of conformer IV (Figure 4), at 40, 50, 78, 128, 140, 157, 206, 222, 256, 270, 301, 418 and 440 cm^{-1} ion internal energies. Figure 5 displays the harmonic vibrational modes obtained at the UMP2/cc-pVDZ level for the D_0 state of conformer IV.

TABLE 2: Frequencies (in cm^{-1}) and Assignments of the Vibrational Bands Observed in the MATI Spectrum of Conformer IV of BB

peak position	ion internal energy	intensity[a]	assignment	UMP2/cc-pVDZ
69872	0	s	IE	
69912	40	vw	τ_{side}	42
69922	50	w	τ_a	52
69950	78	m	B_{C7}	85
70000	128	m	$B_{C7} + \tau_a$	
70012	140	w	T_{CH_3}	129
70029	157	w	$B_{C7} + \tau_{side}^2$	
70078	206	s	β	219
70094	222	s	σ	238
70128	256	vw	$\beta + \tau_a$	
70142	270	vw	$\sigma + \tau_a$	
70173	301	vw	$\sigma + B_{C7}$	
70290	418	m	B_{side}	
70312	440	m	$\beta + \sigma$	

[a] Intensities are denoted as s = strong, m = medium, w = weak and vw = very weak.

TABLE 3: Relative Energies (cm^{-1}) Obtained by Using the Extrapolation Methods for the Conformer I, III, IV and V of Butylbenzene

basis set	BB-I	BB-III	BB-IV	BB-V
ΔE (aug-cc-pVDZ)		24	377	226
ΔE (aug-cc-pVTZ)		40	327	164
ΔE (aug-cc-PVQZ)		67	305	127
ΔE (CBS/aDZ→aTZ)				
A	2.051	2.048	2.054	2.057
B	3.022	3.023	3.024	3.023
total		43	309	143
total + ZEPC[a]		89	306	113
ΔE (CBS/aTZ→aQZ)				
A	2.856	2.854	2.858	2.860
B	4.083	4.078	4.086	4.089
total		84	291	103
total + ZEPC[a]		130	289	73

[a] Zero point energies in this table were calculated at the MP2/cc-pVTZ level.

The MATI spectrum of conformer IV of BB (Figure 4) shows a strong similarity to the spectrum of conformer V of BB.[14] Three prominent vibrational features at 78, 206 and 220 cm^{-1} ion internal energy are therefore assigned as B_{c7}, β and σ, respectively. Because conformer IV displays C_1 symmetry, the intensity of the symmetry forbidden mode of τ_a, barely seen in the C_s conformer V, is now greatly enhanced and observed at 50 cm^{-1}. In addition, the other pure alkyl chain torsion mode τ_{side} is observed at 40 cm^{-1}. This mode is unique to this conformer because it does not appear in MATI spectra of the other three isomers. In addition, two pure alkyl chain modes appear, the methyl group rotor mode at 140 cm^{-1} and the bending mode B_{side} at 418 cm^{-1}, which are in line with appearance of 150 and 402 cm^{-1} in MATI spectrum of conformer III.

Unlike the conformer III spectrum, which displays strong separation of alkyl side chain modes, aromatic ring modes and a lack of combination features, the MATI spectrum of conformer IV shows similar combination patterns to conformer V: Combinations of the B_{C7} mode, $B_{C7} + \tau_a$ and $B_{C7} + \tau_{side}^2$ appear at 128 and 157 cm^{-1}, respectively. Combinations of the σ mode with τ_a and B_{C7} are observed at 270 and 301 cm^{-1}. Finally, a bend and torsion combination, $\beta + \tau_a$, can be recognized at 256 cm^{-1}. Table 2 presents a list of the spectral features

TABLE 4: Absolute Energies (E_h) and $D_0 \leftarrow S_0$ Ionization Energies (IE) Obtained from the MP2/cc-pVDZ Level Calculations for Conformers I, III, IV and V of Butylbenzene

		BB-I	BB-III	BB-IV	BB-V
S_0/E_h (Hartree)	RMP2	−388.236153	−388.235590	−388.234687	−388.235490
	ZEPC	0.214881	0.215084	0.214833	0.214716
	RMP2+ZEPC	−388.021272	−388.020506	−388.019854	−388.020774
D_0/E_h (Hartree)	UMP2	−387.909144	−387.908406	−387.908668	−387.909233
	ZEPC	0.218948	0.218856	0.218920	0.218983
	RMP2+ZEPC	−387.690196	−387.689550	−387.689748	−387.690250
	$\langle S^2 \rangle$	0.867	0.867	0.868	0.867
IE (cm^{-1})	theoretical	72663	72636	72449	72541
	experimental	70148	70146	69872	69955

observed in the MATI spectrum of conformer IV (Figure 4) with assignments.

4.3. Energetics of conformer I, III, IV and V of *n*-Butylbenzene. Though our REMPI and MATI experimental results give accurate electronic transition energies for $S_1 \leftarrow S_0$ and $D_0 \leftarrow S_1$, it is still not possible to deduce the relative energies of the S_0, S_1 and D_0 states because of lack of experimental data to reveal the energetics of the S_0 state.[33] One way to obtain this crucial information is to use highly accurate extrapolation of *ab initio* calculations as stated in section 3. The relative energy results obtained by using an augmented basis set are listed in Table 3. The total energy of BB-I in the S_0 state is used as the origin point compared to the other isomers because it shows the highest stabilization energy for all levels of calculation. Compared with BB-I, for single point (SP) energy calculations (aDZ, aTZ and aQZ), both BB-IV and BB-IV *anti*-isomers show a decrease of relative energies with increasing basis set, and *gauche*-isomer BB-III exhibits the opposite trend. Here, we are not able to determine the reason for these trends. It is unclear whether, with increasing basis set, *anti*-isomers show an increase of stabilization energy or the BB-I isomer becomes relatively less stable due to the increase of repulsion between the aromatic ring and the alkyl side chain.

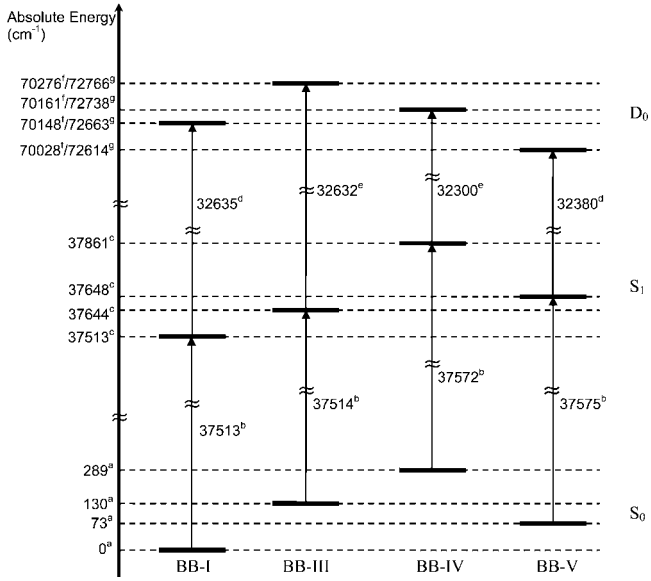

Figure 6. Schematic energy level diagram of four BB conformers illustrating the relative conformer energies in the S_0, S_1 and D_0 states. The values are in cm^{-1}. (a) is calculated at the MP2/CBS(aTZ→aQZ) level of theory, (b) is from REMPI spectra at ref 13, (c) is calculated from (a) and (b), (d) is from MATI spectra at ref 13, (e) is from MATI spectra in this work, (f) is ionic state energy resulting from the calculated S_0 energy (a) + measured two-photon transition energies (b, c, d) and (g) is the calculated ionic stated energy from (a) and the UMP2/cc-pVDZ level of theory for D_0 state.

The extrapolation results are also presented in Table 3. For both the aDZ→aTZ and the aTZ→aQZ extrapolation, *A* and *B* are similar among all isomers at each level. This indicates that the employed extrapolation method is likely to be geometry independent but level related. We also observe that the use of an augmented basis set results in a lower relative energy for BB-III compared to BB-V for all single point energy calculations. In aDZ→aTZ extrapolation, the results show the same trend. Without zero point energy correction, the aTZ→aQZ extrapolation indicates that BB-III is still more stable than BB-V by 19 cm^{-1}. All these values are not in line with the earlier REMPI spectrum which tells us that BB-I and BB-V are the most stable isomers.[14] Only when combined with zero point energy correction, the correct order for all four isomers can be obtained. With 73 cm^{-1} above the BB-I, the BB-V conformer indeed appears as the second most stable conformer, the BB-IV conformer has the highest relative energy of 289 cm^{-1} and in between BB-III has energy 130 cm^{-1} above conformer BB-I. In our earlier study, based on thermodynamics, we obtained an energy difference between BB-I and BB-V of 38 cm^{-1}.[14] This value agrees well with our present calculation at the MP2/CBS(aTZ→aQZ) level. Furthermore, the energy ordering of these four isomers is consistent with the observed signal intensities in the earlier reported REMPI spectrum, for which the conformer of higher relative energy is less populated, resulting in a lower intensity in the REMPI spectrum. We also notice that the aDZ→aTZ extrapolation does not provide a better result compared to single point energy calculation at the aQZ level. This can be explained by the fact that the aDZ basis set is unbalanced, and this affects the accuracy of the aDZ→aTZ extrapolation.[17,28] From our theoretical calculations, we are not able to determine the potential energy barriers between these four conformers. However, because the differences between them come mainly from the geometric structure of the side alkyl chain, one can expect the barrier height to be around 12 kJ/mol, which is much lower than the thermal energy of the molecule at room temperature. This barrier height also means that the different conformations rapidly interchange at room temperature but they can be trapped in the cold molecular beam.

As stated in section 3, the zero point corrected theoretical $D_0 \leftarrow S_0$ ionization energies (IE) can only be calculated at the MP2/cc-pVDZ level in this work. These calculations give us a good relative order of the conformer ionization energies, despite a common overestimation in absolute terms (~3.6%). Table 4 lists the calculated results. The IE of conformer IV corresponds to the lowest value both theoretically and experimentally, and the order of IE(conformer I) > IE(conformer III) > IE(conformer V) > IE(conformer IV) is in perfect agreement with calculated and spectroscopic results. Note that the energy differences between the various IE features are also well reproduced by the calculation. An energy level diagram for these four isomers is shown in Figure 6, illustrating the agreement of

our study for both theory and experiment. In this figure, both $S_1 \leftarrow S_0$ and $D_0 \leftarrow S_1$ transition energies are given as obtained from the REMPI and MATI experimental results and the relative energy of the S_0 state is obtained by the CBS extrapolation method at the MP2/CBS(aTZ→aQZ) level of theory. Combining the theoretical calculations with experimental results the relative energetics for the S_1 and D_0 states have be calculated and displayed in Figure 6.

5. Further Discussion

Although there is no doubt that the major influence on the relative energy of BB isomers is the steric hindrance of the different side alkyl chain geometry, there is a noticeable noncovalent interaction playing an important role in the energetics of BB conformers. BB-I is more stable in the S_0 than BB-V (which has the most straight extended side alkyl chain) because of the stabilizing interaction between the hydrogen atoms and the aromatic ring.[14] This can also explain why BB-III is more stable than BB-IV in the S_0 state, considering that both of them have distorted side chains.

In Figure 6, one may notice that in the S_0 state, BB-V is more stable than BB-III, but this order is reversed in the S_1 state. Actually, both *gauche*-isomers have lower energy than both *anti*-isomers BB-IV and BB-V. This is because with the more expanded electron density in the electronic excited state, the noncovalent interaction between the side chain and aromatic ring becomes even stronger; therefore the *gauche*-isomer is more stable compared for the *anti*-isomer which exhibits less noncovalent interaction.

Once BB is ionized, the attractive interaction between the aromatic ring and the side alkyl side in the neutral states turns into repulsion. The stronger interaction the conformer has, the higher the total energy can be. This is indeed reflected by the relative energies of the cationic states as seen in Figure 6. Conformer V shows the lowest relative energy and is 120 cm^{-1} lower than BB-I in the D_0 states, whereas it is 73 and 135 cm^{-1} higher than BB-I in the S_0 and S_1 states, respectively. The highest energy conformer for the neutral states, BB-IV, has a significantly lower relative energy for the D_0 states as well. BB-IV is no longer the least stable conformer and is 125 cm^{-1} lower in energy than BB-III. It is clear that both *anti*-conformers become more stable in the cationic state compared to the neutral states due to the lower repulsion interaction between the side alkyl chain and the aromatic ring.

According to the above discussion, it is concluded that for the BB monomers, noncovalent interaction plays an important role for the energetics although there is only a very subtle geometrical difference between the four conformers. The noncovalent interactions within the BB monomer conformers change dramatically with electronic state and ionization and show a strong impact on the relative energies of conformers.

References and Notes

(1) Müller-Dethlefs, K.; Hobza, P. *Chem. Rev.* **2000**, *100*, 143.
(2) Pirani, F.; Maciel, G. S.; Cappelletti, D.; Aquilanti, V. *Int. Rev. Phys. Chem.* **2006**, *25*, 165.
(3) Sudha, R.; Kohtani, M.; Jarrold, M. F. *J. Phys. Chem. B* **2005**, *109*, 6442.
(4) Vaden, T. D.; Lisy, J. M. *J. Phys. Chem. A* **2005**, *109*, 3880.
(5) Zhang, C. Y. *J. Phys. Chem. A* **2006**, *110*, 14029.
(6) Hobza, P.; Zahradnik, R.; Müller-Dethlefs, K. *Collect. Czech. Chem. Commun.* **2006**, *71*, 443.
(7) Suzuki, K.; Ishiuchi, S.; Sakai, M.; Fujii, M. *J. Electron Spectrosc. Relat. Phenom.* **2005**, *142*, 215.
(8) Georgiev, S.; Neusser, H. J. *J. Electron Spectrosc. Relat. Phenom.* **2005**, *142*, 207.
(9) Choi, K. J.; Kim, S. K.; Ahn, D. S.; Lee, S. *J. Phys. Chem.* **2004**, *108*, 11292.
(10) Chervenkov, S.; Karaminkov, R.; Braun, J. E.; Neusser, H. J.; Panja, S. S.; Chakraborty, T. J. *Chem. Phys.* **2006**, *124*, 234302.
(11) Kimura, K. *J. Electron Spectrosc. Relat. Phenom.* **2000**, *108*, 31.
(12) Dessent, C. E. H.; Müller-Dethlefs, K. *Chem. Rev.* **2000**, *100*, 3999.
(13) Tong, X.; Černý, J.; Müller-Dethlefs, K. *J. Phys. Chem. A* **2008**, *112*, 5872.
(14) Tong, X.; Ford, M. S.; Dessent, C. E. H.; Müller-Dethlefs, K. *J. Chem. Phys.* **2003**, *119*, 12908.
(15) Ford, M. S.; Tong, X.; Dessent, C. E. H.; Müller-Dethlefs, K. *J. Chem. Phys.* **2003**, *119*, 12914.
(16) Dickinson, J. A.; Joireman, P. W.; Kroemer, R. T.; Robertson, E. G.; Simons, J. P. *J. Chem. Soc. Faraday Trans.* **1997**, *93*, 1467.
(17) Halkier, A.; Helgaker, T.; Jorgensen, P.; Klopper, W.; Koch, H.; Olsen, J.; Wilson, A. K. *Chem. Phys. Lett.* **1998**, *286*, 243.
(18) (a) Martin, J. M. L.; Taylor, P. R. *J. Chem. Phys.* **1997**, *106*, 8620. (b) Truhlar, D. G. *Chem. Phys. Lett.* **1998**, *294*, 45.
(19) Truhlar, D. G. *Chem. Phys. Lett.* **1998**, *294*, 45.
(20) Jurecka, P.; Hobza, P. *J. Am. Chem. Soc.* **2003**, *125*, 15608.
(21) Haines, S. R.; Geppert, W. D.; Chapman, D. M.; Watkins, M. J.; Dessent, C. E. H.; Cockett, M. C. R.; K. Müller-Dethlefs, M. C. R. *J. Chem. Phys.* **1998**, *109*, 9244.
(22) Ford, M. S.; Haines, S. R.; Pugliesi, I.; Dessent, C. E. H.; Müller-Dethlefs, K. *J. Electron Spectrosc. Relat. Phenom.* **2000**, *112*, 231.
(23) Gunzer, F.; Grotemeyer, J. *Int. J. Mass Spectrom.* **2003**, *228*, 921.
(24) Dessent, C. E. H.; Haines, S. R.; Müller-Dethlefs, K. *Chem. Phys. Lett.* **1999**, *315*, 103.
(25) Gerstenkorn, S.; Luc, P. Atlas Du Spectre D'absorption De La Molecule D'iode, Orsay (France), 1978.
(26) Chupka, W. A. *J. Chem. Phys.* **1993**, *98*, 4520.
(27) Frisch, M. J.; Trucks, G. W.; Schlegel, H. B.; Scuseria, G. E.; Robb, M. A.; Cheeseman, J. R.; Montgomery, J. A., Jr.; Kudin, K. N.; Burant, J. C.; Millam, J. M.; Iyengar, S. S.; Tomasi, J.; Barone, V.; Mennucci, B.; Cossi, M.; Scalmani, G.; Rega, N.; Petersson, G. A.; Nakatsuji, H.; Hada, M.; Ehara, M.; Toyota K.; Fukuda R.; Hasegawa J.; Ishida M.; Nakajima T.; Honda Y.; Kitao, O.; Nakai H.; Klene M.; Li X.; Knox J. E.; Hratchian H. P.; Cross J. B.; Adamo C.; Jaramillo J.; Gomperts R.; Stratmann R. E.; Yazyev O.; Austin A. J.; Cammi R.; Pomelli, C.; Ochterski, J. W.; Ayala, P. Y.; Morokuma, K.; Voth, G. A.; Salvador, P.; Dannenberg, J. J.; Zakrzewski, V. G.; Dapprich, S.; Daniels, A. D.; Strain, M. C.; Farkas, O.; Malick, D. K.; Rabuck, A. D.; Raghavachari, K.; Foresman, J. B.; Ortiz, J. V.; Cui, Q.; Baboul, A. G.; Clifford, S.; Cioslowski, J.; Stefanov, B. B.; Liu, G.; Liashenko, A.; Piskorz, P.; Komaromi, I.; Martin, R. L.; Fox, D. J.; Keith, T.; Al-Laham, M. A.; Peng, C. Y.; Nanayakkara, A.; Challacombe, M.; Gill, P. M. W.; Johnson, B.; Chen, W.; Wong, M. W.; Gonzalez, C.; Pople, J. A. *Gaussian 03*, version C.02; Gaussian, Inc.: Wallingford, CT, 2004.
(28) Černý, J.; Tong, X.; Hobza, P.; Müller-Dethlefs, K. *J. Chem. Phys.*, in press.
(29) Chewter, L. A.; Sander, M.; Müller-Dethlefs, K.; Schlag, E. W. *J. Chem. Phys.* **1987**, *86*, 4737.
(30) Lu, K. T.; Eiden, G. C.; Weisshaar, J. C. *J. Phys. Chem.* **1992**, *96*, 9742.
(31) Sato, S.; Byodo, K.; Kojima, T.; Shinohara, H.; Yanagihara, S.; Kimura, K. J. *J. Electron Spectrosc. Relat. Phenom.* **2000**, *112*, 247.
(32) Takahashi, M.; Kimura, K. *J. Chem. Phys.* **1992**, *97*, 2920.
(33) In ref 14, the relative intensity of the $S_1 0°$band origins of isomer I and V were used to calculate relative energy difference. This approach was not used here due to the large errors that would be incurred for the low intensity isomer III and V band origins.

JP710997Q